

PEDESTRIAN COLLISIONS WITH FLAT-FRONTED VEHICLES: INJURY PATTERNS AND IMPORTANCE OF ROTATIONAL ACCELERATIONS AS A PREDICTOR FOR TRAUMATIC BRAIN INJURY (TBI)

Feist, Florian

Gugler, Jürgen

Vehicle Safety Institute, Graz University of Technology
Austria

Arregui-Dalmases, Carlos

del Pozo de Dios, Eduardo

López-Valdés, Francisco

European Center for Injury Prevention, Universidad de Navarra
Spain

Deck, Caroline

Willinger, Rémy

University of Strasbourg, IMFS-CNRS
France

Paper Number 09-0264

ABSTRACT

Research on pedestrian protection currently is focusing mainly on passenger cars. However, impacts with heavy goods vehicles (HGV) and buses are also important, especially in urban areas and in developing countries. This study is an attempt to show the distribution of injury patterns focused on the head injury mechanism. In the European project APOLLO WPII database with a number of 104 pedestrians injured by a HGV or bus were identified. The head was found the most severely injured anatomic region, with an average AIS of 3.1, followed by the abdomen/pelvis (AIS 2.9), and the thorax (AIS 2.1). Using the Dr. Martin transformation matrix, head injury mechanisms were assigned to codified head injuries. Around 69% of the sustained head injuries had a rotational injury mechanism, 21% translational, and 10% either. Three multi-body vehicle models, representing two HGV and one bus, were used in a large parameter analysis. The simulations showed that the angular velocity change is exceeding 30rad/s and the angular acceleration is exceeding 10.000rad/s² in simulations where the HIC value was below 1000. Additionally the head injury risk was assessed by prescribing the accelerations of the human pedestrian model's head to a finite element head and brain model. It can be concluded that head injuries are the most frequent injuries sustained by pedestrians involved in a collision with a flat-fronted vehicle and rotational accelerations are responsible for around 70% of head injuries. Impactors currently used in pedestrian protection regulations do not assess rotation-induced injuries.

Keywords: Vulnerable Road Users, Pedestrian, Bicyclist, Heavy Goods Vehicles, Trucks, Head Injuries, Rotational accelerations, FE head/brain model

MOTIVATION

In numerical studies conducted in the project APROSYS [1], [2], [3] the interaction between vulnerable road user and heavy goods vehicle were studied by means of finite element vehicle models (IVECO Stralis and generic short-haul goods vehicle) and finite element and multi-body pedestrian models (pedestrian accident compliant (PAC) model and Madymo human pedestrian models). The numerical studies highlighted threatened and highly loaded body regions [1].

In parallel the HV-CIS injury and accident database was analysed by Smith [4]. The accidentology pointed out, that the head is the most frequently (seriously) injured body region. Other studies proof the same [5].

The numerical studies, however, did not show the relevance of head injuries to that extent. It was therefore assumed, that the secondary contact with the ground leads to the large number of head injuries. The secondary impact (with the ground) was not investigated in the previously mentioned studies.

In 2008 a workshop organised by APROSYS SP2 was held in Neumünster, Germany. There, Arregui [6] pointed out that head injuries in accidents between pedestrians and flat front vehicles are more frequently due to rotation (rotational acceleration/velocity) than due to translation.

It therefore seemed worthwhile to rerun the numerical simulations and pay attention to the head rotation and the secondary impact (with the ground). In collaboration with APROSYS SP5 (biomechanics) the head injury risk was re-evaluated using a finite element head/brain model.

Eventually, the findings of the numerical studies were compared with the field data of the injury database APOLLO.

INTRODUCTION

Very little research has been carried out so far in the field of pedestrian collisions involving HGV. Most studies performed are focusing on passenger cars, and LTV (light truck vehicle).

Graz University of Technology and the University of Strasbourg were involved in the EC funded project APROSYS. Sub-project 2 initiated research in the field of HGV-VRU accidents, investigated the interaction of vulnerable road users (VRU) with heavy goods vehicles (HGV) in experiment and in a numerical environment and came up with a so-called aggressivity index (HVAI) assessing the risk imposed by a HGV on vulnerable road users. Sub-project 5, Biomechanics, developed improved head injury criteria based on a finite element head-brain model by reconstructing 68 accident case results (6 motorsport, 22 football player, 29 pedestrian and 11 motorcycle accidents) [7]. This model is capable of assessing the potential head injury risk in road safety and distinguishing between contusion, sub-dural haematoma (SDH), skull-fracture, and diffuse axonal injuries (DAI).

The European Center for Injury Prevention was involved in the European Project APOLLO, in the Work Package II, investigating the injuries associated to the hospital discharges in Europe. Work-package II, "The burden of injuries in the EU: indicators and recommendations for prevention and control", is coordinated by the University of Navarra [8]. The "core" project consists on the development of report on the burden of (non-fatal) injuries in the European Union. The APOLLO database stores the information of 1.085.673 cases from the hospital discharges, of which some 74.660 cases are traffic-related injuries.

HEAD INJURY MECHANISMS

Many experiments and studies on head impact have been carried out to investigate the head's mechanical response properties. In general, the impact response was described in terms of head acceleration, impact force and intracranial pressure.

Translational accelerations

The pioneer of the experimental studies in this field was Holburn (1943) [9]. He worked on tangential stresses in a gel model, observing that the rotation between skull and brain could explain most of the traumatic brain injuries. It was noted that translations were not as harmful as rotations; an amazing conclusion that is still valid nowadays.

Profound research has been carried out on impact tolerance of human head sponsored by the automotive industry. The first approach to human tolerance limits was introduced by Gurdjian in 1953 [10] and Lissner et al in 1960 [11], and it is widely known as the Wayne State Tolerance Curve (WSTC). Figure 1 reproduces that curve.

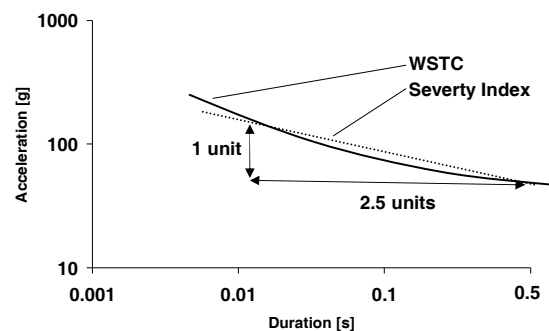


Figure 1: Severity Index, based on [12]

The WSTC indicates a relationship between average translational anterior-posterior acceleration level and duration of the acceleration pulse that accounts for similar head injury severity in head contact impacts. Gurdjian and colleagues assumed that measuring the tolerance of the skull to a fracture was equivalent to measuring the tolerance to a brain injury.

Combinations of acceleration level and pulse duration that lie above the curve are assumed to exceed human tolerance, and will cause severe irreversible brain injury. Combinations below the curve do not exceed human tolerance.

In 1966 Gadd [12] introduced the SI (Severity Index) based on WSTC studies. It was calculated by integrating the linear acceleration and raised to the power of 2.5 (the slope of curve expressing the WSTC in log t– see Figure 1). Gadd indicated an acceptable maximum value of 1000.

Using the WSTC and the criteria developed thereafter, restrictions that arise from the test conditions have to be considered. The major limitations are the shortage of data of initial curve points, the accelerometer position located in the back of the head (far from the centre of gravity) and techniques for scaling the animal data and the supposed correspondence of skull fracture and brain injury. Bearing in mind that WSTC is based on direct

frontal impact tests, the result should not be applied to other impact directions.

In 1971, Versace ^[13] proposed an alternative formulation of the Severity Index, subsequently proposed by the US National Highway Traffic Safety Administration (NHTSA) and included in the FMVSS 208. This injury criterion is called HIC (Head Injury Criterion) – see (1):

$$HIC = (t_2 - t_1) \left[\frac{\int_{t_1}^{t_2} a_r dt}{t_2 - t_1} \right]^{2.5} \quad (1)$$

Where a_r is the resultant linear acceleration measured at head centre of gravity (in G's) and t_1 and t_2 are two arbitrary times (in s).

To determine the relationship between HIC and injuries to the skull and brain, available test data were analysed statistically by fitting normal, log normal, and two parameter Weibull cumulative distributions to the data set, using the maximum likelihood method to achieve the best fit for each function ^[14]. The best fit of the data was achieved with the log normal curve.

A major limitation of the HIC - not taking into account rotational acceleration - is often criticized. Another common limitation is the lack of a relationship between human head injury and the acceleration response measured with anthropomorphic test devices that is the transformation function between the dummy and the cadaver.

Nevertheless, the HIC is the index of cerebral damage most commonly accepted by the scientific community and the only value that the automotive industry uses to develop new vehicles or to fulfil regulations.

The a3ms (or cum3ms) criterion is also based on the WSTC, and it is defined as the maximum acceleration level obtained for an impact-duration of 3 ms, where any three milliseconds window should not exceed 80 g in the resultant acceleration curve. This requirement has also been incorporated in European and American regulations.

Rotational accelerations

In experimental studies using animals by Unterharnscheidt and Higgins ^[15], angular accelerations were applied to primates' heads. They could reproduce subdural haematoma, bridge veins ruptures between skull and brain, as well as brain injuries and spinal cord injuries.

Ommaya ^[16] carried out a study with 25 monkey squirrels, in which they induced and compared pure translational motions with combinations of rotational and translational accelerations, determining the reduction of the resistance in case of combined

motion - despite being smaller in intensity. It was also found that the angular acceleration and the according injury thresholds are related to the mass of the brain. The tolerance limit for human beings was obtained by scaling the results from the primate test.

In 1993, working on rotational acceleration as an injury mechanism, Melvin ^[17] determined human being's tolerance to angular acceleration in 7500 rad/s² with a concussion probability of 99%. In 1974 Löwenhielm suggested that the bridging veins between skull and brain started to tear from 400 rad/s² angular acceleration or a change of angular speed from 70 rad/s ^[18].

Margulies and Thibault ^[19] proposed a criterion to produce a Diffuse Axonal Injury (DAI) according to the Angular Acceleration and the Delta Angular Speed, which is reproduced in Figure 2.

The area below the curve indicates the head acceptable limit for two different brain weights (500g, 1400g). The solid black curve indicates the tolerance for the human brain.

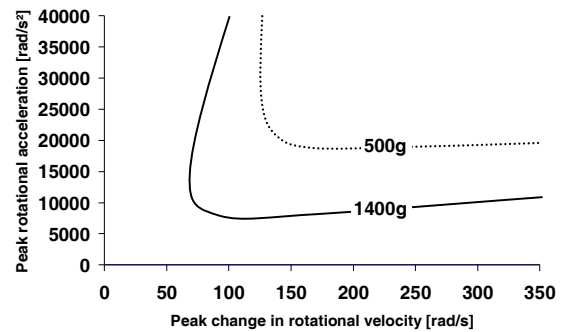


Figure 2: Rotational acceleration and rotational velocity as injury mechanism, based on ^[19]

Table 1 shows tolerance values commonly used. However, additional studies on volunteers suggest that much higher tolerance values may be possible for short durations.

Table 1.
Tolerance thresholds for rotational acceleration and angular velocity. [20]

Tolerance threshold, 50% probability	Type of brain injury	Reference
$\alpha = 1800 \text{ rad/s}^2, \Delta t < 20 \text{ ms}$	Cerebral concussion	Ommaya et al., 1967
$\omega = 30 \text{ rad/s}, \Delta t > 20 \text{ ms}$	Rupture of bridging veins	Löwenhielm et al., 1975
$\alpha < 4500 \text{ rad/s}^2, \Delta t < 20 \text{ ms}$	Brain surface shearing	Advani et al., 1982
$\alpha < 3000 \text{ rad/s}^2$		
For $\omega < 30 \text{ rad/s}$:		
AIS 5; $\alpha > 4500 \text{ rad/s}^2$		
For $\omega > 30 \text{ rad/s}$:		
AIS 2; $\alpha > 1700 \text{ rad/s}^2$	General injury	Ommaya et al., 1984
AIS 3; $\alpha > 3000 \text{ rad/s}^2$		
AIS 4; $\alpha > 3900 \text{ rad/s}^2$		
AIS 5; $\alpha > 4500 \text{ rad/s}^2$		

In an attempt to combine translational and rotational acceleration, Newman in 1986 [21], in contact with Transport Canada, introduced the concept of generalized GAMBIT (Generalized Acceleration Model for Brain Injury Tolerance). The model attempts to weight, in an analogous manner to the principal shear stress theory, the effects of the two forms of motion. The GAMBIT equation is as follows:

$$G(t) = \left[\left(\frac{\alpha(t)}{a_c} \right)^m + \left(\frac{\alpha(t)}{a_c} \right)^n \right]^{\frac{1}{s}} \quad (2)$$

Where $a(t)$ and $\alpha(t)$ are the instantaneous values of translational and rotational acceleration respectively. a_c and a_c are limiting critical values and n , m and s are empirical constants selected to fit the available data from Kramer and Appel field accident database [22]. ($n = m = s = 2.5$, $a_c = 250g$, $\alpha_c = 25.000 \text{ rad/s}^2$). These values were more or less confirmed in a more recent publication [23]. $G=1$ is set to correspond to a 50% probability of MAIS 3.

Using simulations of the injuries sustained by passengers in documented automobile accidents, the severity / probability relationship shown in Figure 3 was generated [21] These have not been fully validated but may serve as basis for future development.

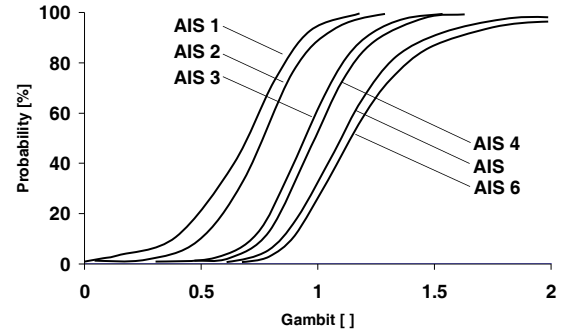


Figure 3: Head injury severity probability as a function of GAMBIT criterion [21]

The GAMBIT has been criticized on the grounds that it does not take into account any time related aspect of head injury process. That is, it only depends on maximum values and does not invoke any particular limit of velocity change or time duration of acceleration exposure. Another weak point of this criterion is its inadequate validation.

The HIP (head impact power) is a more global approach to a head protection criterion [24]. The formula is the sum of power terms for all rotational and translational degrees of freedom – see (3) -and is based on the hypothesis that head injuries do occur if a certain rate of kinetic energy change is exceeded. A threshold value of 12.79 kW (kNm/s) is proposed for 50% of concussion, a mild traumatic brain injury where unconsciousness [25] may occur (see Table 2).

$$HIP = \sum_{i=1}^3 m a_i \int a_i dt + \sum_{i=1}^3 I_{ii} \alpha_i \int \alpha_i dt \quad (3)$$

Table 2.
Relationship between HIP and probability for concussion [25]

Probability for concussion	HIP [kW]
5%	4.7
50%	12.79
95%	20.88

Gennarelli et al. [26] presented a set of interrelationships between biomechanical metrics and the entire spectrum of DBI (Diffuse Brain Injury), and the first hypothesis of the potential influence of a generic factor on human tolerance to trauma. The main limitation of this study is the simplification used in presenting the tolerance hypothesis, assuming that just the angular acceleration is responsible for the DBI (when it is commonly accepted that duration of acceleration and angular velocity are also required).

Table 3 represents the connection between rotational acceleration and Diffuse Brain Tolerance related to

the Abbreviated Injury Scale (AIS) – as found by Gennarelli et al. [26].

Table 3.
Relationship between rotational acceleration and AIS, based on [26]

AIS	Rotational Acceleration [rad/s ²]
1	2878
2	5756
3	8633
4	11511
5	14389

At this time, no rotational criteria have been approved by the scientific community or adopted by the automotive industry.

Currently, the FE models are gradually becoming more sophisticated and they have the potential for understanding the complex injury mechanism of head impact. And the scientific community aggress in exploring this new tool to increase the knowledge the head injury field.

METHOD

Earlier numerical studies showed that the injury risk of a certain body region depends largely on the vehicle size and initial position of the VRU with respect the HGV [27]. In these studies, however, different codes and numerical pedestrian models were used. Therefore, it was difficult to draw consistent conclusions.

Instead of using different numerical models of vehicle and pedestrian, one parameterisable multi-body vehicle model was developed. Three front shape geometries (short-haul HGV: MAN L2000, long-haul HGV: IVECO Stralis and one bus: MAN Lion) were used for the analysis of head-injuries and later for the front-shape optimization based on a generic-algorithm. The bus geometry was included in order to be consistent with the analysis of the APOLLO injury database, which does not allow for a discrimination of bus and truck.

The numerical study is conducted in three steps:

1. The three breed models were used to analyse the head acceleration (rotation/translation) and head rotation velocity. Additionally a number of parameters were varied to find the maxima and minima of the simulation outputs. Parameter that have been varied:
 - Friction between HGV and VRU: 0.2 ... 0.4
 - Friction between Shoes and Ground: 0.5 ... 0.7
 - Friction between VRU and Ground: 0.4 ... 0.75
 - Facing direction of pedestrian: +60° ... -60°

- Start of braking: -1s ... 0.2s
 - Initial velocity: 30 ... 40 km/h
 - Pedestrian gait: 10 postures
 - Ground-Clearance of the vehicle: depending on vehicle model
2. In a further step, the secondary impact (with the ground) was studied. Finally head accelerations in primary and secondary impact are compared.
 3. The three breed models were used in a generic algorithm aiming to reduce the objective function. The objective function is a combination of head injury risk evaluation (rotation and translation) and thorax injury risk evaluation. Weighting factors are based on the findings of the accidentology. (To be described in another publication to come).
 4. Accelerations measured in the COG of the pedestrian's head were prescribed to a finite element head/brain model. That model was used to assess the risk for brain injuries. The evaluation is compared to the results obtained by applying "conventional" injury criterions
 5. The APOLLO database was analysed. Head injuries related to an accident with a heavy goods vehicle or bus were distinguished in rotational acceleration induced injuries and translational acceleration induced injuries.

Numerical Vehicle Model

Multi-body framework of vehicle - The vehicle consists of four major rigid bodies (see Figure 4):

1. Two rigid bodies representing the unsuspended mass of the rear and front axle. The front axle is connected to the reference body (the ground) by a translational joint (front axle) and a restraint (rear axle). The front and rear axle are supporting the chassis. Spring-damper elements account for the suspension of the vehicle.
2. The chassis is bearing the bumper and the front underrun protection (the lower bumper).
3. The cabin is bearing the remaining front (grill, hood, windshield frame and windshield). The cabin is suspended by a planar joint (and restraints in x- and z-direction) and a free joint (and a restraint in z-direction).
4. Other rigid bodies are supporting the contact surfaces (ellipsoids or facet surface) of the vehicle front. A marginal mass and inertia is assigned to these rigid bodies.

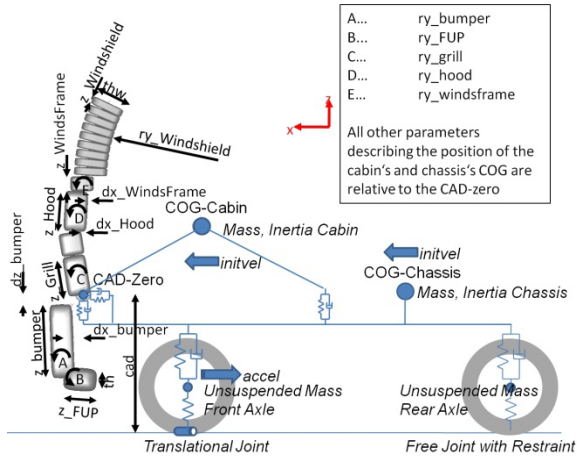


Figure 4: Multi-body framework of the HGV model

Geometry

The geometry of the vehicle (the phenotype) can be defined by a number of parameters (the genotype) [28]. Generally the front shape is defined by the following parameters:

- Height of facet surface and ellipsoid (z_name)
- Rotation of facet surface and ellipsoid in relation to parent ellipsoid (ry_name)
- Offset of facet surface and ellipsoid in relation to parent surface (dx_name)

In total a string of 18 numerical parameters defines the geometry.

Using initial scaling, the facet surfaces (e.g. the facet surface for the bumper) are scaled accordingly to the parameter z_name . As a result the mesh size changes from one vehicle to the other. The initial element size was chosen such that the maximal effective element-size is not exceeding 5x10mm (as long as the value of z_name is not exceeding a predefined value).

Three reference models were created, to fit the front shape of a short-haul truck, a long-haul truck and a bus (see Figure 5).

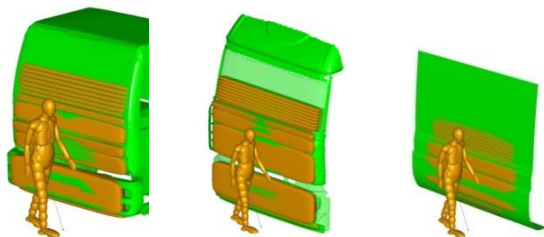


Figure 5: The three breed models

Contact Pedestrian – Vehicle

The initial truck model was built up by ellipsoids. Initial simulations showed up the deficiencies of the

ellipsoid contact for the analysis of the primary contact with the truck: The MB-MB contact does not take into account the shape of the contact partners and gaps between the ellipsoids might cause body parts to be braced. Generally the contact involving at least one ellipsoid (the human body) has a major drawback: As soon as the penetration is exceeding the semi-axis, contact forces are inverted.

The stress-based FE-MB contact shows drawbacks as well. Failure of materials (e.g. windshield) can not be modelled directly, but by a work-around. Facet models are less CPU time efficient. Hysteresis model 3, where “[...]the unloading curve is shifted and scaled without using a hysteresis slope [...]” [29] is not available and again: as soon as the penetration is exceeding the ellipsoid’s semi-axis, the contact-force is inverted.

Still, the advantages of FE-MB contact with a stress-based contact model prevail for the analysis of the primary contact (which is the contact with the truck front). For the analysis of the secondary contact (which is the contact with the ground), the ellipsoid HGV model was used, since less CPU time is needed for rather long simulation durations. The sub-chapters below describe briefly the particular issues considered with the contact interaction of the ellipsoid HGV model and the facet HGV model.

Multi-body-Multi-body (MB-MB) contact

The ellipsoid HGV model and consequently the MB-MB contact were used in the study of the secondary impact (pedestrian to ground contact). No contact characteristics were assigned to the HGV ellipsoids. The contact type was referring to the characteristics of the pedestrian model. The vehicle was assumed to be non-compliant. This assumption is fair for the analysis of the secondary contact.

For the contact with the ground the contact type “combined” was used.

Multi-body-Finite Element (FE-MB) contact-

By a switch in the input file, the user can select between the ellipsoid HGV model and the facet surface HGV model. The FE-MB stress based contact requires the force-penetration functions (as they are normally used in MB-MB contacts) to be transformed into stress-strain functions (or in fact a stress-penetration functions, when the thickness of the null-shells is selected to be 1m).

A force-penetration $F(e)$ curve is given from quasi-static or dynamic testing. The shape of the penetrating body is given and can be approximated by an ellipsoid. That ellipsoid (master surface) is impacting a flat facet surface (slave surface). The stress as a function of the penetration (contact thickness =1m) can be calculated in the following

manner: The nominal penetration is $e_j = \Delta e_j$, where Δe is the step-width of the numerical solution and j the number of the step. The penetration of node i at timestep j is p_{ij} . The area associated to each step is A_j . For a sphere with a radius r the area associated to a newly penetrating node i^* is $A_{i^*j} = \pi [(2r e_j - e_j^2) - (2r e_{j-1} - e_{j-1}^2)] / \cos(\alpha_{i^*j})$ where α_{i^*j} is the angle between the vector from node i to the centre of the ellipsoid and the vertical at time j (see Figure 6).

For node 1, which always has the largest penetration (p_{1j}) of all penetrating nodes, the stress σ_{1j} is calculated such that the formula $F(e) = \sum \sigma_{ij}(p_{ij}) A_i$ is met. For all other nodes the stress σ_{ij} is interpolated from previous steps j . A simple visual basic macro implemented in MS Excel is solving that problem numerically with a step-width $\Delta e = r/100$.

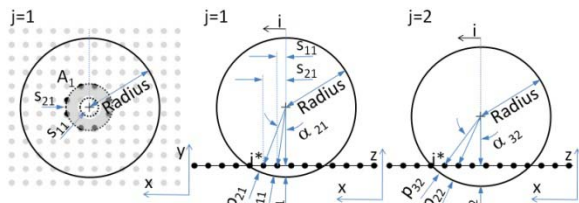


Figure 6: Approach for converting the force-deflection curves to stress-strain curves for slave nodes intruding into a master surface

Some body parts of the vulnerable road user are penetrating deeply into the truck front, such as into the grill area or into the windshield when this is failing. Two approaches were chosen as work-around:

- The struck-side arm, hand and shoulder ellipsoid were converted into a facet surface
- A multi-layered surface was chosen to model the windshield and the grill

The windshield is modelled by up to three layers of facet surfaces (there are only two layers required for the windshield close to the windshield frame, three layers are required more to the centre of the windshield, see Figure 7). The first layer is for simulating the glass itself, while the second and third layer is for simulating the laminate (the polyvinyl butyral film). The second layer has an offset of 7mm. As soon as the contact force between the intruding surface and second windshield layer exceeds a certain threshold value, the contact with the first windshield layer is turned off. By doing so, the failure (the cracking) of the windshield can be simulated. The third layer has an offset of about 60mm to the second layer, which is a little less than the half-diameter of the adult pedestrian's head. This is to prevent contact force inversion, when an ellipsoid is intruding by more than its semi-axis. The third layer is inactive for facet-facet contacts (with the shoulder and the arm).

It was assumed, that the failure of the windshield affects any following contacts with the windshield. Example: Is the pedestrian's shoulder contacting the second layer of the windshield (which can be the case, when the pedestrian is hit by a flat front vehicle with a low windshield, e.g. a bus) and the contact force is exceeding a predefined force level (about 200-700N), the first layer's contact is turned off. That in turn means that any body part (e.g. the head) impacting the windshield later than the shoulder is never intercepted by the first layer. This was found a reasonable assumption, when looking to impactor tests of the windshield, where the circumferential and in particular the "spider-web" cracks propagated well beyond the outer dimensions of the intruding body.

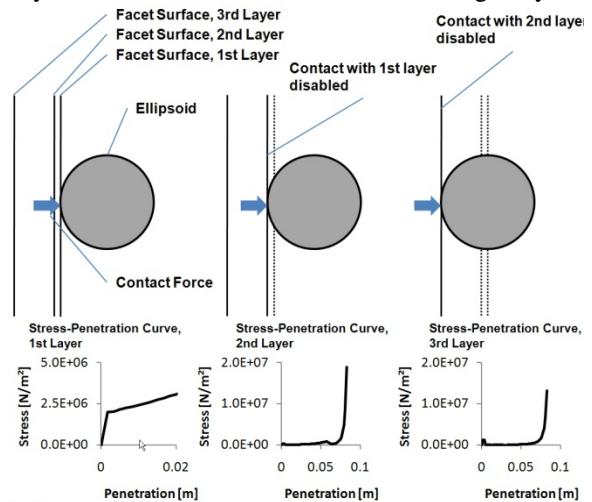


Figure 7: Three layered windshield model

This approach was found to be very effective for simulating the failure of the windshield or generally non-monotonously increasing force-deflection characteristics. Figure 7 shows the modelling of the windshield. Figure 8 shows a comparison between the given force-deflection curve of a dynamic impactor test and the model response of the three layered windshield model.

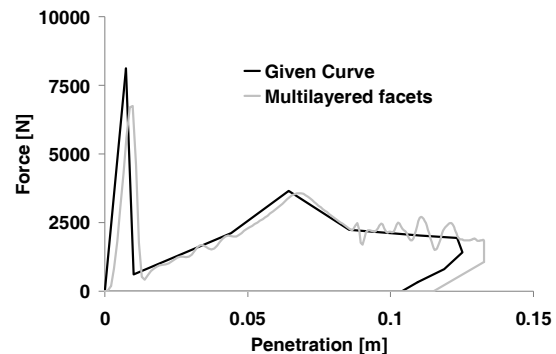


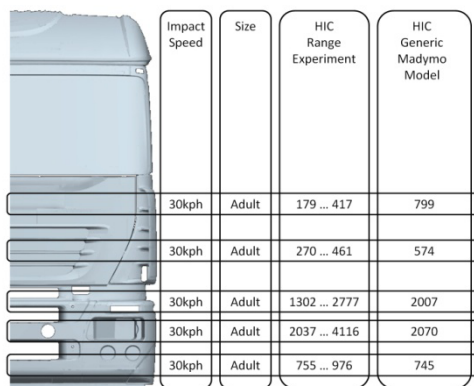
Figure 8: Three layered windshield model

The grill area is modelled by two layers. The second layer is to model the more rigid parts behind the grill-like the radiator.

Stress-Penetration Characteristics

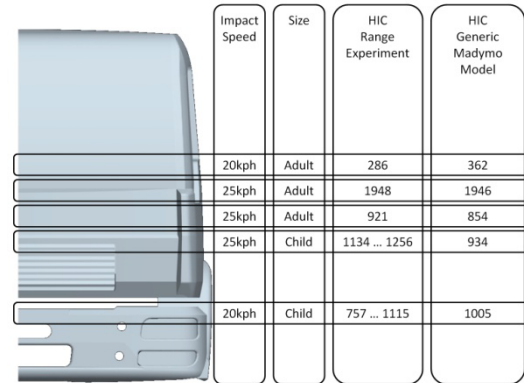
It was assumed that the windshield of a HGV is comparable in terms of force-deflection to a windshield of a passenger car. Hence, the force-deflection characteristics as obtained by Mizuno [30] and used in other publications on pedestrian accident simulation [31] were applied to the HGV windshield. Two experimental tests of the windshield impacted by an EEVC WG17 adult hemisphere were available. A comparison with the response of the numerical model showed a fair correlation. The first experimental test was performed at 20kph, leading to a HIC of 286. A similar point selected on the windshield of the numerical model led to a HIC of 362. A second test, performed at 25kph showed a HIC of 756 in the experiment and 848 in the numerical simulation.

Most of the contact characteristics of the generic multi-body trucks are based on the quasi-static measurements of the IVECO Stralis front [32]. These characteristics have been assigned to the front of the three reference models. Dynamic impact tests of the MAN L2000 and IVECO Stralis front with adult and child EEVC WG 17 head impactors were available [33], too. Finally, the performances of the generic multi-body models have been compared with the results of these dynamic tests – see Figure 9 and Figure 10.



Impact Speed	Size	HIC Range Experiment	HIC Generic Madymo Model
30kph	Adult	179 ... 417	799
30kph	Adult	270 ... 461	574
30kph	Adult	1302 ... 2777	2007
30kph	Adult	2037 ... 4116	2070
30kph	Adult	755 ... 976	745

Figure 9: Performance of generic Madymo model, long-haul HGV [32]



Impact Speed	Size	HIC Range Experiment	HIC Generic Madymo Model
20kph	Adult	286	362
25kph	Adult	1948	1946
25kph	Adult	921	854
25kph	Child	1134 ... 1256	934
20kph	Child	757 ... 1115	1005

Figure 10: Performance of generic Madymo model, short-haul HGV [33]

Friction Characteristics

In pedestrian accident reconstructions, Ziegenhain [34] found a friction-coefficient of 0.2 between pedestrian and vehicle appropriate in almost all accidents. Deviations are marginal. However, the values may get larger in form-locking cases (e.g. where the pedestrian's clothes are caught by the wiper or other protruding parts).

Same value was used by Wood et al. [35], [36]. A slightly higher value (0.25) was used by Yoshida [37]. IHRA used a value of 0.3 [38].

In a recent study by Untaroiu [39] a value of 0.4 was used. In the present study a friction between 0.2 and 0.4 was used.

Contact Pedestrian - Ground

Force-Deflection Characteristics

Stevenson [40] referred to values given by Chadbourn et al. [41] and used these values in a sensitivity analysis of the HIC response to the ground stiffness, Stevenson used values from 2.6 kN/mm (lowest value from Chadbourn et al.), over 40 kN/mm (mid-range value from Chadbourn) up to 10.000 kN/mm (extremely stiff-approximately equivalent to a solid steel road). Finally an infinitely stiff road was assumed, where only the head's force-deflection characteristics were used for the calculation of the head accelerations. Stevenson concluded, that the "[...] ground stiffness values only need to be of the correct order of magnitude to ensure reasonable results [...]".

Davich et al. [42] examined the mechanical properties of 36 soil specimens from six subgrade soil samples. The specimens were different with respect to confinement and moisture content. The young's modulus reached from 129 MPa (having a poisson's ratio of 0.4) up to 958 MPa (with a poisson's ratio of 0.36). The poisson's ratio in all soil specimens ranged from 0.18 up to 0.40.

Salem et al. [43] studied the asphalt concrete modulus of 11 freeze and non-freezing sites in the US. At a mid-depth temperature of 20°Celsius, the young's modulus reached from 8800 to 14000 MPa in the samples from non-freezing sites, and from 3800 to 7000 MPa in those from freezing sites. Overall the values reached from 1600 up to 22500 MPa.

In another publication, Nessnas [44] set up a numerical model of a pavement, where a young's modulus of 3745 MPa, 7490 MPa and 14980 MPa and a Poisson ratio of 0.35 for the wearing course were assumed.

Using Hertz's Formulas [45] for spheres impacting a flat plate, the force deflection curves were calculated. The following values were used:

- The head was assumed to be a sphere with a diameter of 165mm.
- For soil-grounds, a young's modulus of 129 and 958 MPa (according to Davich [42]) was assumed
- For roads with an asphalt wearing course, a stiffness of 1600, 3750, 7490, 14980 and 22500 MPa (according to Nessnas and Salem [44], [43]) was assumed.
- Additionally three Poisson's ratios were used 0.18, 0.35 and 0.4 (according to Davich and Nessnas [42], [44]).

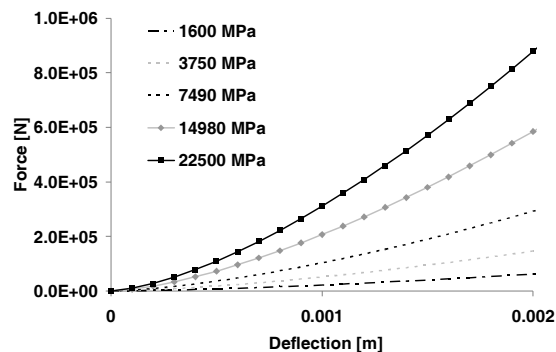


Figure 11: Force-deflection curve for roads with asphalt course (poisson's ratio = 0.35)

For a penetration of 2mm (see Figure 11), the linear stiffness of the road is in between 2.5kN/mm (soil) and 30 to 440 kN/mm (asphalt). These values are correlating very well with the linear stiffness used by Stevenson [40].

Friction Characteristics

Two coefficients of friction are needed for the contact between pedestrian and ground: one for the contact between the shoe sole and the ground and another one for the contact between the pedestrian's body and the ground.

For the contact between shoes and ground, Simms and Wood [46], [36] used a value of 0.58. Sacher [47] reported a coefficient of friction of 0.5 (for turf). Stevenson [40] used a value of 0.7 in the numerical study.

Table 4 summarizes the values reported in various studies on the coefficient of friction, showing a range from 0.37 to 0.75. These values do not apply for the friction with the shoe sole.

In previous numerical studies the upper range of these values was applied: Yoshida [37] used a friction-coefficient of 0.67. The same value was used by IHRA [38]. In a recent study by Untaroiu [39] a friction coefficient of 0.6 was applied.

Table 4. Coefficient of Friction Pedestrian-Ground [46], [40]

Source	Surface	n	Range	Mean
Becke, Golder	Asphalt, wet	15	0.43-0.53	0.47
Becke, Golder	Asphalt	30	0.50-0.72	0.63
Kuhnel	Asphalt	4	0.52-0.67	0.54
Sturtz	Asphalt	8	0.40-0.74	0.57
Lucchini	Asphalt	16	0.37-0.51	0.43
Severy	Asphalt	15	0.40-0.75	0.66
Searle (1983)	Asphalt			0.66
Severy (1966)	Asphalt		0.45-0.60	
Fricke (1990)	Concrete		0.40-0.65	
Wood (1988)	Asphalt		0.57-0.58	
Searle (1983)	Grass			0.79
Fricke (1990)	Grass		0.45-0.70	

Numerical Human Model

Posture

Earlier studies by Anderson et al [48] showed that the walking posture of the pedestrian influences kinematics and injury outcomes.

IHRA [38] conducted a parameter study with multi-body pedestrian models in three walking positions (corresponding to a six stance sequence). A more recent study by Untaroiu [39] describes an accident reconstruction based on optimisation techniques and taking into consideration a number of initial postures. Based on 10 stances of the gait cycle, functions for H-point height and joint-angles were approximated, allowing for a continuous stance sequence.

Based on curves published in the study by Untaroiu [39], a sequence of ten gait cycles for the 50th percentile human pedestrian model was developed. The hip-angle (the curve published by Untaroiu [39] for the hip seems to be corrupted) was changed properly, to fit the pictures of the gait cycle (and the angles of the ankle) published in the same.

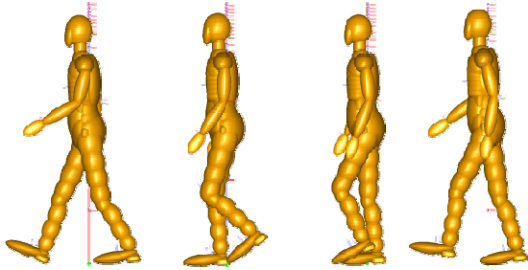


Figure 12: Gait Cycle

Table 5 summarizes initial joint positions as set in the numerical simulations. In pre-simulations (where all major joints except for the human joint were locked) the H-Point was altered such that the contact force between floor and shoes (contact characteristics of the shoes were used) amounted for about 730-740N. The human body's joints were locked at simulation start. A logic switch (connected to a contact sensor) is unlocking all joints as soon as there is a contact force between HGV and the pedestrian. The free joints between shoes and feet were kept locked throughout the simulations.

Table 5.
Initial Joint Positions for a continuous sequence of gait

Stride	0%	10%	20%	30%	40%
H-Point	0.872	0.901	0.915	0.919	0.911
Hip left	0.201	0.178	-0.279	-0.454	-0.470
Hip right	-0.413	-0.282	-0.200	0.018	0.175
Knee left	0.342	0.840	1.120	0.871	0.255
Knee right	0.093	0.093	0.327	0.120	0.156
Ankle left	-0.349	-0.205	-0.082	0.090	0.115
Ankle right	0.049	0.041	0.041	0.000	-0.100
Shoulder left	-0.171	-0.112	0.034	0.190	0.295
Shoulder right	0.329	0.261	0.138	0.011	-0.125
Elbow left	-0.817	-0.727	-0.545	-0.443	-0.386
Elbow right	-0.352	-0.352	-0.352	-0.611	-0.733
Neck low	-0.400	-0.400	-0.400	-0.400	-0.400

Design of Experiments

Three breed models (a long-haul and a short-haul traffic truck front and a bus) have been used in the numerical simulations. Beside of the front geometry the following parameters have been varied:

- Friction: HGV and VRU: 0.2 ... 0.4
- Friction: Shoes and Ground: 0.5 ... 0.7
- Friction: VRU and Ground: 0.4 ... 0.75
- Facing direction of pedestrian: +60° ... -60°
- Start of braking: -1s ... 0.2s
- Initial velocity: 30 ... 40 km/h
- Pedestrian gait: 10 postures
- Ground-Clearance of the vehicle: depending on vehicle model

The software ModeFrontier Version 4.1.0 by Esteco was used for the design of experiments (DOE). The

experiments are based on a random sequence. The software fills the design space (bounded by the values mentioned above) randomly, with a uniform distribution. The randomly generated simulations are used to analyse the head accelerations (rotation/translation) and associated injury criteria.

Finite Element Head Model

Model

Conventional head injury predictors such as HIC cannot predict the risk for injuries due to rotational accelerations. Also, they fail in distinguishing the types of injuries to the head, as there are:

- Skull-fractures: Fractures of the skull can be comminuted, depressed – due to local forces, leading to inward displaced bones - or linear – due to widely distributed forces.
- Subdural (SDH) or subarachnoid haematoma (SAH): Injuries to the vasculature, leading to bleeding between brain and skull (subdural) or under the arachnoid membrane, which covers the brain and spinal cord (subarachnoid).
- Diffuse axonal injuries (DAI): Extensive lesions in white matter tracts, leading in most cases to unconsciousness and persistent vegetative state. 90% of all patients suffering a severe DAI never regain consciousness [49].

Furthermore, conventional head injury predictors are insensitive to the direction of force/acceleration imposed to the head.

A finite element skull-brain model overcomes these deficiencies. Currently there are a number of such finite-element models available. These models differ from each other with respect to the number of elements, ranging from the 10 to the 300 thousands, and the anatomic details modelled.

- WSUBIM: The Wayne State University brain model consists of approx. 320.000 elements and represents a 50th percentile male human head with a mass of 4.3 kg. It was used extensively for the reconstruction of sports accidents, resulting in concussions.
- SIMon: The simulated injury monitor FEM head model was initially developed by DiMasi et al. [50] and extended by Eppinger, Takhounts and Bandak [51], [52]. It represents a 50th percentile male human head with a mass of 4.7 kg. The model has less than 10.000 elements.
- KTH: A head-neck model developed by Kleiven and Hardy [53].
- UCDBTM: The University College Dublin Brain Trauma Model was created by Horgan and Gilchrist [54]. The influence of number of elements on the model response was investigated,

by varying the element density from 9000 to 50000 elements. Also, the model is scalable with respect to size, weight and thickness of the CSF.

In the present study, the Strasbourg University Finite Element Head Model (SUFEHM) head model was used. The model was initially developed by Kang et al. [55] in 1997. The SUFEHM head model has approx. 13.000 elements. It represents a 50th percentile male human head with a mass of 4.7 kg. First tolerance limits for that head model were identified by Willinger and Baumgartner [56]. Further improvements to the model's geometry were initiated by Deck et al. [57]. More tolerance limits were identified by the reconstruction of 68 accidents [7].

By contrast to other models, e.g. SIMon, the skull is non-rigid, made of a three-layered composite shell. In order to reproduce the overall compliance of cranial bone, a thickness in combination with an elastic brittle law were selected for each layer with a Tsai-Wu criterion. The cerebral spinal fluid filling the space between the brain and the skull is made of brick elements using an elastic material. The brain is modelled by brick elements using a visco-elastic material model [58] (see Figure 13).

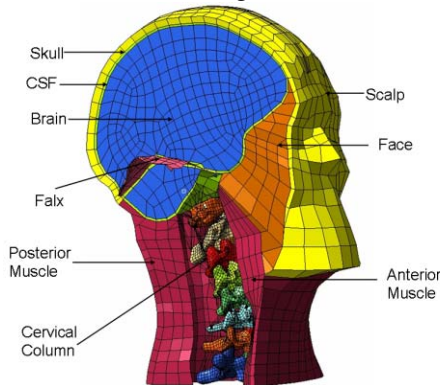


Figure 13: Section of SUFEHM

The SUFEHM injury predictors

Based on the simulation of 68 well documented accidents with occurrence of head trauma, tolerance limits for the SUFEHM head model have been identified within APROSYS SP5 [7], [59]. Using logical regression techniques, tolerance limits have been identified by comparing the FE model response and the reported injuries.

Diffuse axonal injuries were further distinguished by severity: Mild (or moderate) diffuse axonal injuries (DAI) assigned to AIS 2 or 3 and severe DAI assigned to AIS 4+.

With the help of the regression, tolerance limits for three types of injuries (fracture, SDH, DAI) were established. The mechanical parameters constituting

the tolerance limits refer to a risk of 50% (see Table 6) for the respective injury [7].

Table 6.
Tolerance limits for 50% risk of injury used in FE simulation [7]

Injury	Mechanical Parameter	Tolerance limits
Skull fracture	Strain Energy, Skull	865 mJ
Subdural or subarachnoid haematoma	Min. Pressure Spinal Fluid	-135 kPa
	Strain Energy, Spinal Fluid	4211 mJ
Mild diffuse axonal injury	Von Mises Stress, Brain	26 kPa
	Von Mises Strain, Brain	0.25
	First Principle Strain, Brain	0.31
Severe diffuse axonal injury	Von Mises Stress, Brain	33 kPa
	Von Mises Strain, Brain	0.35
	First Principle Strain, Brain	0.40

Analysis of Apollo Database

One of the biggest challenges in head injury is to identify the injury mechanisms leading to a certain injury type. One of the main hypotheses of this study is to assume that rotational accelerations have a great influence in the case of pedestrians involved in an accident with a flat front vehicle.

Martin et al [60] analysed the different AIS codes for head injury, and classified these codes by injury mechanisms: Injuries induced by rotational acceleration, translational acceleration and either (when the injury could be produced by rotational and/or translational acceleration). Table 16 (in the Annex) shows an excerpt of the matrix by Martin which classifies the head injury codes by their injury mechanism.

To evaluate the influence of the rotational acceleration in the APOLLO database a new variable has been included. The Martin transformation matrix has been implemented in the database to evaluate the presence of the different injury mechanisms.

RESULTS

Multi-body Simulations

Results are separated by primary impact (the impact of the pedestrian with the front of the vehicle) and secondary impact (the impact of the pedestrian with the ground). For the calculation of the HIP (head impact power), the following values were applied: Mass = 4.69kg, $I_{xx}=0.02\text{kgm}^2$, $I_{yy}=0.0222\text{kgm}^2$, $I_{zz}=0.0145\text{kgm}^2$. These values are consistent with the values applied in the human pedestrian model supplied with Madymo. When referring to HIC, the HIC 36ms is meant.

Primary Impact

Statistical parameters of the 300 numerical simulations are summarized in Table 7. The table shows the mean value and the quartiles (25th, 50th and 75th percentile) for the peak rotational/translational acceleration, head injury criterion (HIC), cumulative 3ms criterion (cum3ms), Gambit (G) and head impact power (HIP).

The median value of the HIC is only slightly above the widely applied threshold value of 1000. The median Gambit suggests a rather low risk for head injuries. The HIP, which is used to assess the risk for concussion, is exceeding the 50% probability value for concussion (12.8kW). The median cum3ms value is clearly above 80g.

Table 7.
Mean and statistical dispersion of the numerical simulation – Primary Impact

	Peak head acceleration		HIC	3ms	G	HIP
	[rad/s ²]	[g]				
Mean	9605	195	2999	136	0.82	90
25 th p.	5329	93	477	87	0.40	30
50 th p.	7848	156	1022	114	0.64	55
75 th p.	11616	225	2041	160	0.95	83

Table 8 distinguishes the results by vehicle type. Clearly the short-haul truck is leading to the worst results. That is also in line with the findings of previous studies, where full finite element models were used to study the interaction between vulnerable road users and HGV [27].

Table 8.
Median by vehicle type – Primary Impact

	Peak head acceleration		HIC	3ms	G	HIP
	[rad/s ²]	[g]				
All	7848	156	1022	114	0.64	55
s. HGV	11919	216	1756	159	0.89	79
l. HGV	6642	117	835	108	0.59	40
Bus	6452	92	577	87	0.40	31

s. HGV = short-haul HGV, l. HGV = long-haul HGV

Secondary Impact

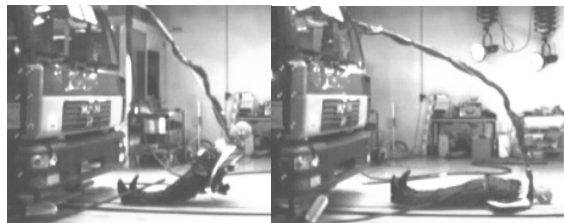


Figure 14: Hybrid III impacting the floor

Previous experimental tests with a standing Hybrid III [2] dummy have shown that the secondary contact is extremely critical with respect to loading of the

head. A HIC of 17600 to 33900 was found in four tests (see Figure 14). Peak head accelerations reached up to 1170g.

The numerical simulations show similar results. Statistical parameters of 300 numerical simulations are summarized in Table 11. A median (50th percentile) head rotation acceleration (peak) of 66 krad/s² and a translational acceleration of 870g was found. These high accelerations come along with extremely high criterions: a HIC of 20500, a cum3ms of 430g and a Gambit of 4.

Table 9.
Mean and statistical dispersion of the numerical simulation – Secondary Impact

	Peak head acceleration		HIC	3ms	G	HIP
	[rad/s ²]	[g]				
Mean	69285	809	21013	398	3.82	444
25 th p.	44552	553	6850	284	2.75	240
50 th p.	66292	866	20527	434	4.10	406
75 th p.	91976	1026	29122	499	4.74	605

Still, cases were found with very low criterions: About 5% of simulations show uncritical HIC, 3ms, Gambit and HIP criterion values.

A very severe case was selected for a sensitivity analysis of the ground stiffness. A linear force-deflection curve was assumed. Results are shown in Table 13. Starting from 40kN/mm, there was a relatively limited influence of different orders of magnitude of ground contact stiffness on the resulting injury criteria. Soil grounds (2.6kN/mm), however, led to completely different results with respect to injury criteria.

Table 10.
Sensitivity to stiffness of ground

Stiffness [kN/mm]	Peak head acceleration [krad/s ²]	HIC [10 ³ g]	G	HIP [kW]
2.6	36.9	5.1	13641	2.1
40	59.4	11.8	46503	4.8
60	61.2	12.4	49930	5.1
100	62.6	12.8	51591	5.3
10.000	67.9	13.9	56827	5.7

Finite Element Simulation

Nine out of 300 numerical simulations have been selected for a more detailed analysis with a FEM head model. Angular and translational accelerations measured in the multi-body simulations of the primary impact were prescribed to the SUFEHM head model. The acceleration curves were pre-filtered with CFC-1000.

Besides assessing these nine cases with the SUFEHM head model, conventional injury predictors, such as the HIC (head injury criterion), the GAMBIT (Generalised Acceleration Model for Brain Injury

Threshold), the cum3ms (the accumulative 3 milliseconds acceleration) and the HPC (Head power criterion) – see Table 11 – were applied, too.

The simulations are:

- (1) A 50th percentile, ellipsoid male human pedestrian model in walking posture is hit on the left side by the generic facet heavy goods vehicle model having the geometry and the characteristics of an IVECO Stralis. The cabin pivot is 950mm above ground. The vehicle is travelling at 40kph.
 - (2) A 50th percentile, ellipsoid male human pedestrian model in walking posture is hit on the left side by the generic facet heavy goods vehicle model having the geometry of a MAN L2000. The cabin pivot is 870mm above ground. The vehicle is travelling at 40kph.
 - (3) Like ID 2, however, cabin pivot 930mm above ground
 - (4) Like ID 2, however, cabin pivot 800mm above ground
 - (5) Like ID 2, however, cabin pivot 1080mm above ground
 - (6) Like ID 2, pedestrian turned about the z-axis such that the pedestrian is approaching the truck front at 45°.
 - (7) Like ID 6, however, cabin pivot: 800mm above ground
- Finally two simulations were performed with a 50th percentile facet male occupant model in standing posture
- (8) hit on the rear by a finite element heavy goods vehicle model having the geometry and the characteristics of a MAN L2000. The cabin pivot is 930mm above ground. The vehicle is travelling at 40kph.
 - (9) Like ID 8, however, hit on the left shoulder. Cabin pivot 830mm above ground. The vehicle is travelling at 30kph.

Table 11 summarizes the characteristics of the selected cases.

Table 11.
Characteristics of selected cases

ID	Peak head acceleration [rad/s ²]	HIC [g]	G []	cum3ms [g]	HIP [kW]	
1	6327	108	817	0.47	102.3	41.9
2	4520	88	366	0.38	66.1	33.7
3	8562	146	700	0.64	100.3	67.1
4	11423	269	1958	1.11	86.3	103.9
5	7416	135	1090	0.58	132	51.9
6	22841	410	4915	1.65	197.6	122.8
7	6428	191	1864	0.76	160.8	70.8
8	2730	151	1613	0.6	138.1	68.2
9	2672	74	359	0.3	70	22.1

By applying the expanded Prasad-Mertz ^[61] curves and it's counterpart for the Gambit (see Figure 3), the

risk of head injuries associated to the HIC and Gambit were summarized in Table 12.

Table 12.
Conventional injury predictors and the associated risk for injury

ID	Risk of Head injury related to the HIC [%]		Risk of Head injury related to the Gambit [%]	
	Moderate	Severe	Moderate	Severe
1	77	9	9	0
2	22	2	4	0
3	64	6	31	<3
4	100	87	91	71
5	93	22	<3	<3
6	100	100	100	1
7	100	82	0.74	8
8	99	65	22	<3
9	21	2	<3	0

Table 13 and Table 14 summarize the risk for specific head injuries as predicted by the SUFEHM head model. In six out of nine cases under study a risk greater than 50% for severe DAI and SDH is predicted.

Table 13.
Injury predictors calculated by SUFEHM head and the associated risk for injury – Part A

ID	Von Misses stress Brain [kPa]	Risk of diffuse axonal injury [%]	
		Moderate	Severe
1	39.5	100	88
2	39.5	100	88
3	51	100	99.9
4	74	100	99.9
5	44.6	100	98
6	52	100	99.9
7	31.4	100	38
8	16.1	<1	0
9	12	<1	0

Table 14.
Injury predictors calculated by SUFEHM head and the associated risk for injury – Part B

ID	Minimum pressure Spinal Fluid [kPa]	Risk of subdural haematoma [%]
	1	-126
2	-126	34
3	-145	66
4	-166	90
5	-151	75
6	-177	98
7	-159	84
8	-114	18
9	-68	<1

Analysis of Apollo Database

The APOLLO database contains 1.085.673 cases from the hospital discharges, of which 74.660 are traffic related injuries (8 European countries codify including the injury mechanism). This subgroup

comprises 10.341 pedestrians. Taking into account only cases that were codified according to the International Classification of Diseases (ICD 10) [62] 3.786 pedestrians remain, of which 104 are pedestrians involved in an accident with Heavy Good Vehicles.

HGV or bus versus pedestrian

Table 15 was obtained by analyzing the APOLLO database and classifying the injuries by body region and nature (Barell injury matrix) [63]. Remark: Table 15 shows only an excerpt of the results (the original table contains a total of 252 injuries).

Table 15.
Barell injury matrix for pedestrian involved in HGV collision (excerpt)

Type of Injury	Fracture	Internal	Open wound	Contusion/superficial	Crush	%	AIS
Traumatic brain injury	17	58	4	0	6	37%	3.14
Thorax	14	12	0	4	0	12%	2.14
Abdomen, pelvis, trunk	17	4	0	2	6	12%	2.91
Lower extremity	24	0	18	4	0	21%	1.87
TOTAL	102	74	25	12	12	100%	

It can be observed that the most frequently injured area is the head with 37% of all injuries, followed by lower extremities 21%, thorax 12%, and the abdominal/pelvic area 12%.

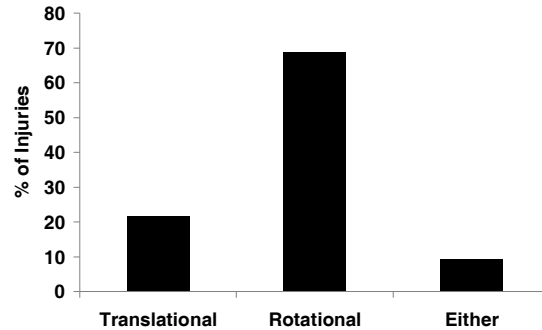
Compared with the injuries sustained for pedestrians involved in passenger car collisions in case of survival, the results are different: According to Yang et al [64] the most frequently injured area was found the lower extremities with 32.4% of all injuries, followed by the head (26%), the abdominal/pelvic area (12%), and the thorax (5.5%).

To evaluate the influence of the rotational acceleration in the APOLLO database a new variable has been included. The Martin transformation matrix [60] has been implemented in the database (see excerpt in Table 16) to evaluate the presence of the different injury mechanisms.

From the 93 head injuries only 74 could be matched with the AIS code or matrix to be included in the study. All of the not classifiable were categorised as minor injuries (AIS 1), so there is no loss of information for moderate or more severe injuries (AIS 2+).

Figure 15 shows that just 21% of all head injuries analyzed have the translation acceleration as a single

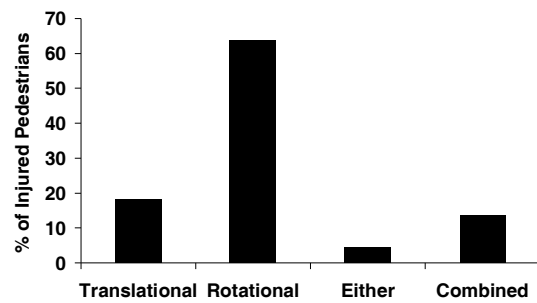
injury mechanism, in 69% of all cases rotational acceleration is the only injury mechanism, and in 10% of the cases rotational or translational acceleration can be responsible for the head injury.



Source: APOLLO n =104 pedestrians, N=74 head injuries

Figure 15: Head injuries by injury mechanism (HGV or bus versus pedestrian)

Following the methodology developed by Martin et al. examining all 104 pedestrian cases individually, all the head injuries have been re-processed with the transformation matrix, analyzing all the different combinations of Translational, Rotational or Either. Some of the codes show up several times while others never appear at all. Cases where a single pedestrian sustains two or more types of head injuries, a “combination” is assigned – see Figure 16. From initial 104 injured pedestrians only 44 sustained head injuries that can be processed with the Martin matrix. From these pedestrians only 8 had sustained head injuries solely due to translational acceleration, 28 due to rotational acceleration, 2 pedestrian had head injuries due to rotational or translational acceleration and 6 due to a combination of injury mechanisms.



Source: APOLLO n =44 pedestrians, N=74 head injuries

Figure 16: Injured pedestrians and injury mechanism (HGV or bus versus pedestrian)

Rotational acceleration is clearly more frequent as the translational acceleration in the case of pedestrian accident. The large presence of “combined” as an

injury mechanism is due to the immense number of injuries sustained by some pedestrians, making it very unlikely that all injuries are assigned to one single injury mechanism.

Passenger car versus pedestrian

The results are considerably different from the figures reported in the literature: Pedestrians involved in a crash with a passenger car ^[65] (see Figure 17) only 17% sustain head injuries due to rotational accelerations. Another 17% sustain injuries solely induced by translational accelerations, 38% either and 28% due to combined mechanisms (data from the Pedestrian Crash Data Study PCDS). The percentage in motorbike accidents is quite similar: 5% for translational, 13% for rotational, 34% for either and 48% in case of combined [60].

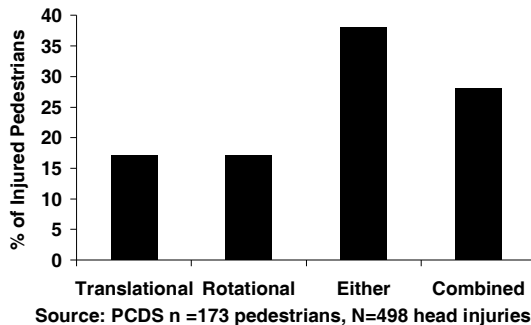


Figure 17: Injured pedestrians and injury mechanism (Passenger car versus pedestrian)

DISCUSSION

Multi-body Simulations

Considering the median values found in the study of the primary impact, the findings of previous studies were confirmed: The HIC is rather uncritical. The peak head rotational accelerations (median value for all flat front vehicles: 7848 rad/s²) can be assessed more critical, when applying the values found by Genarelli [26] or Ommaya ^[66]. The same applies to the median value of the cum3ms, which is clearly above 80g. Also the HIP is clearly exceeding the level of 12.8 kW (50% probability of concussion). A median Gambit, of 0.64 was found for all vehicles under study, which is equivalent to 25% probability of AIS 2 head injuries.

The study showed that the short-haul truck is leading to the worst results with respect to head injury criteria. This is in correlation with the findings of previous studies. While the adult's head is impacting the unforgiving lowermost edge of the windshield of the short-haul truck, the head is intercepted rather

softly by the grill of the long-haul truck. The vehicles, that were inspiring the generic models, are not only different with respect to size. Also, different materials are applied in the design of the front structure. While sheet metal is covering the front of the short-haul truck, almost the complete grill of the long-haul truck is made of fibre reinforced plastics.

For the short-haul truck a Gambit median value of 0.89 was observed, which is equivalent to a 40% probability of AIS 3 injuries. Best results were achieved by the bus.

Secondary Impact

Experimental tests with a standing Hybrid III dummy hit by a MAN L 2000 truck travelling at 30kph showed clearly the severity of the secondary impact. In the four experimental tests the resultant peak head acceleration ranged from 1020g to 1170g, leading to a HIC between 17.600 and 33.900. The Hybrid III pedestrian dummy was facing towards the front of the HG. The situation does not reflect what really happens on the road: In most real-world accidents the pedestrian is hit laterally. The Hybrid III, however, was designed for frontal impact: Hitting the Hybrid III pedestrian dummy laterally will have likely led to damage of thorax and legs and knee joints respectively.

As a result of the initial orientation of the pedestrian, the dummy's back of the head was fiercely hit, when falling to the ground (see Figure 14).

It was expected, that the numerical simulations show less severe head to ground impacts, since the pedestrian model is mostly hit laterally in the numerical simulations. Consequently it was assumed, that the human model hits the ground with its side first. However, in most cases the walking posture of the human model led to a rotation about the pedestrian's vertical axis. Eventually, the pedestrian was hitting the ground with the face or the back of the head. The shoulder did not mitigate the severity of the impacts. As a result injury criteria for the head were extremely high and so is the risk for fatal injuries.

The present study shows clearly that the secondary impact is by far more severe than the primary impact. Pedestrian protection afforded by HG and flat front vehicles need to address the pedestrian post-impact kinematics. Studies by Faßbender [32] indicate that a sort of an aerodynamic front (referred as "nose-cone") is capable of reducing the severity of the secondary impact – beside of reducing the risk for run-over.

Clearly, the problem of the secondary impact exists also with passenger cars. Yang et al. ^[67] noted that if the pedestrian strikes the ground head-first, following a collision with a passenger car, head injuries from

the secondary impact will generally be more severe than injuries related to the primary impact. Otte and Pohlmann^[68] concluded that 56% of all injuries are due to the secondary impact.

The forward projection kinematics of pedestrians hit by a flat fronted vehicle seems to facilitate the severity of the secondary impact. Same was noted by Tanno et al.^[69] and^[70].

In two multibody simulations a facet human occupant model was used, instead of the ellipsoid human pedestrian model. Previous studies showed [27] that the facet model can be used for the very initial phase of the impact. The head-neck kinematics differed significantly: While in the facet model the head showed a distinct translational movement in the very initial phase of the impact (followed by a rotation), the ellipsoid model showed a rotational movement right from the beginning.

Finite Element Simulations

For the simulations with the finite element head model, cases have been selected, where at least one criterion (peak acceleration, HIC, cum3ms or Gambit) was exceeding the given threshold value.

The comparison of injury predictors calculated with the SUFEHM head and “conventional” injury criteria showed that one criterion is not enough for predicting head injuries. According to a regression analysis by Deck^[7], the HIC shows a high correlation to severe DAI and skull fracture. To other injuries (SDH, mild DAI), there is little regression.

The analysis with the FEM head predicts for 6 out of 9 cases under study a very high risk (greater than 50%) for DAI, even in cases where the HIC was well below 1000 (e.g. case ID 2). For six out of nine cases under study a high risk (greater than 50%) for SDH is predicted by the finite element head model.

Analysis of Apollo Database

Clearly the analysis of the Apollo database shows the high relevance of head injuries sustained by pedestrians following a collision with a flat front vehicle. The database also shows the high relevance of head injuries due to rotational accelerations. While in passenger cars hitting a pedestrian the occurrence of head injuries induced by rotational and translational accelerations is almost equivalent, rotation-induced head injuries to pedestrians in HGV and busses are three times more frequent than translation-induced injuries.

A possible explanation for the difference could be the different kinematics in these pedestrian accidents, and also the small sample size used in the present study.

Connecting the findings of the field data with the numerical simulations is not straight-forward, but it can be assumed that head injuries are more likely caused by the secondary contact, as it is the more severe contact, showing extremely high translational and rotational accelerations.

CONCLUSIONS

In a multi-disciplinary approach (using generic multi-body vehicle models, a detailed finite element head/brain model as well as field data from an injury database) it was tried to investigate the relevance of rotation-induced head injuries to pedestrians hit by a large flat front vehicle (a heavy goods vehicle or bus).

The primary and the secondary impact of the pedestrian were investigated by using a parameterisable multi-body vehicle model and a numerical human pedestrian model.

Using DOE software a number of boundary conditions were varied, such as vehicle geometry, gait, orientation of the pedestrian, vehicle speed and friction coefficients. For the study in total 600 numerical simulations were analysed.

Measured head accelerations were evaluated by using HIC, HIP, Gambit and cum3ms. Nine simulations of the primary impact were selected and the measured head accelerations were prescribed to a FEM head model and evaluated by applying the tolerance limits developed for the SUFEHM.

Additionally field data from a European database on hospital discharges was included in the analysis to highlight the relevance of rotation-induced head injuries.

Following conclusions can be drawn

- There is no single injury predictor (like HIC, Gambit, HIP), that can assess the risk for injuries to the head or brain alone. The present study suggests that FEM head models can predict head injuries more reliably and more differentiated, than conventional injury predictors or criteria.
- The secondary impact (with the ground) is a big issue for all vulnerable road-users hit by a vehicle. In particular for flat fronted vehicles, like busses or trucks. Providing a better protection in the primary impact only is not enough. Additionally the post-impact kinematics needs to be considered. These could mitigate the consequences of the ground impact significantly (e.g. by causing a sliding impact of the pedestrian to the ground).
- Future human pedestrian models need a good validation of head rotation kinematics. The use of different numerical models revealed in-consistent

head and neck kinematics, resulting in deviations with respect to rotational accelerations.

- The HIC (Head injury Criterion) is a good indicator for head injuries like severe DAIs or skull fractures in frontal impacts and is a good initial tool to improve pedestrian protection. However this criterion cannot predict all the injuries sustained by a pedestrian. Rotational velocity and rotational acceleration should also be included in the pedestrian criteria in the future; otherwise injuries could be sustained by pedestrians despite a low HIC. The use of FE models to predict brain injuries needs to be the first source of knowledge in the near future. Such models are required to be applicable for any direction of impact.

LIMITATIONS

Multi-body Simulation

For the analysis of the secondary impact (when the pedestrian is hitting the ground) a rigid vehicle was assumed. In the primary impact some of the impact energy will be dissipated by the vehicle. This might slightly change the post-impact kinematics.

Also, the impact speed was assumed to be between 30 to 40kph and only frontal impacts were considered. The data in the Apollo database, however, contain all sorts of HGV-pedestrian accidents including those at lower impact speeds and to the side of the vehicle.

Finite Element Simulation

In this study the SUFEHM is driven by accelerations fields applied at the centre of gravity of the head which skull is supposed to be rigid. In this context no bone fractures can be predicted but similar analysis can be done with a deformable skull by simulating direct impacts. In this case the SUFEHM (deformable skull) is launched - just before impact - with an initial velocity on deformable structures and head injuries can be estimated.

Injury Database

The small number of pedestrian injured by a HGV is the main limitation of this epidemiologic study. The Transformation Matrix have been developed by well know researchers, but some AIS codes could be classified by other researches in a different group.

ANNEX

Table 16.
Excerpt of transformation Matrix [60]

Code	Severity	Type	Code	Severity	Type
113000	6	T	120602	4	R
115099	9	B	121002	5	R
115299	9	B	121004	4	R
115999	7	B	121099	3	B
120202	5	R	121202	4	R
120402	5	R	121299	3	B
120499	5	B	121402	5	R

R – rotation induced, T- translation induced; B- induced by either translation or rotation

REFERENCES

- [1] F. Feist, C. Ciglaric, E. Mayrhofer and H. Steffan. An Interaction Study between Vulnerable Road Users and Heavy Truck Front Structures. 1-14. 22-7-2006. Athens, Greece, Bolton University. ICrash Conference Proceedings 2006.
- [2] F. Feist, R. Puppini, A. Giorda, M. Avalle and J. Gugler. Improvements to the protection of vulnerable road users: retrofittable, energy absorbing front-end for heavy goods vehicles. 1-18. 22-7-2008. Kyoto, Japan, Bolton University. ICrash Conference Proceedings 2008.
- [3] R. Puppini, P. Smeriglio, L. Consano and E. Mayrhofer. Heavy Vehicle Accidents Involving Pedestrians & Cyclists. 2006. Göteborg, Transport Research Arena Europe.
- [4] T. Smith and I. Knight. Summary of UK accident data. AP-SP21-0038. 2005. London, Crowthorne, Transport Research Laboratory (TRL). Unpublished report for the EC-project APROSYS.
- [5] D. Otte and J. Nehmzow. German In-Depth Accident Study (GIDAS): Accidents of commercial vehicles with pedestrian and bicycles. Feist, F. AP-SP21-0074 VRU Workshop Proceedings Praha, 43-54. 23-3-2005. Graz, Austria, Graz University of Technology, Graz. Deliverable report. Published report for EC-project APROSYS.
- [6] C. Arregui. What can be learnt from the introduction of pedestrian protection in passenger cars. AP-SP21-0088, 1-26. 7-5-2008. Navarra, Spain, European Centre for Injury Prevention, University Navarra. Presentation at the APROSYS Workshop held in Neumünster, Germany.
- [7] C. Deck and R. Willinger. Improved head injury criteria based on head FE model. International Journal of Crashworthiness 13 (6), 667-678. 6-12-2008. Oxon, UK, Taylor&Francis.
- [8] APOLLO. Burden of Injuries in the EU: Indicators and recommendations for prevention and control. <http://www.euroipn.org/apollo/WP2.htm> . 10-3-2009. 15-3-2009.
- [9] A. H. S. Holburn. Mechanics of head injuries. The Lancet - Neurology 2, 438-441. 1943.
- [10] E. Gurdjian, H. Lissner, R. Latimer, B. Haddad and J. Webster. Quantitative determination of acceleration and

- intercranial pressure in experimental head injury. *Neurology* 3, 417-423. 1953.
- [11] H.R.Lissner, M.Lebow and F.G.Evans. Experimental studies on the relation between acceleration and intracranial pressure changes in man. 329-338. 1960. surgery, gynecology and obstetrics 111.
- [12] C.Gadd. Use of a weighted - impulse criterion for estimating injury hazard. SAE Paper 660793 . 1966.
- [13] J.Versace. Review of the Severity index. 1971. 15th Stapp Car Crash Conference, SAE.
- [14] E. Hertz. A note on the head injury criterion (HIC) as a predictor of the risk of skull fracture. 37th Annual Proceedings of the AAAM . 1993.
- [15] F. Unterharscheidt and L. S. Higgins. Traumatic Lesions of Brain and Spinal Cord due to Nondeforming Angular acceleration of the Head. *Texas Reports on Biology and Medicine* 27(1), 127-166. 1969.
- [16] A. Ommaya, P. Yarnell, A. Hirsch and Z. Harris. Scaling of experimental data on cerebral concussion on sub-human primates to concussion threshold for men. SAE 670906. 11th Stapp Car Crash Conference , 47-52. 1967.
- [17] J. W. Melvin and W. Lighthall, *Brain-Injury Biomechanics*. In *Accidental Injury*. (Ed. A. M. Nahum and J. W. Melvin) pp. 277-302, 1993.
- [18] P. Löwenhielm. Strain tolerance of the Vv cerebri sup (bridging veins) calculated from head-on collision tests with cadavers. *Z.Rechtsmedizin* 75, 131-144. 1974.
- [19] S. Margulies and L. Thibault. A proposed tolerance criterion for diffuse axonal injury in man. *J.Biomechanics* 25, 917-923. 1992.
- [20] K.-U. Schmitt, P. Niederer and F. Walz, *Trauma Biomechanics: Introduction to Accidental Injury*, pp. 1-174, Swiss Federal Institute of Technology (ETH) and University of Zurich, Zurich 2004.
- [21] J. Newman. A generalized acceleration model for brain injury threshold (GAMBIT). Proceedings of IRCOBI Conference , 121-131. 1986.
- [22] F. Kramer and H. Appel. Evaluation of protection criteria on the basis of statistical biomechanics. Proceedings of IRCOBI Conference , 45-57. 1990.
- [23] J. Newman. Criteria for Head Injury and Helmet Standards. Snell Memorial Foundation Seminar , 1-23. 6-5-2005. Medical College of Wisconsin.
- [24] J. Newman, N. Shewchenko and E. Welbourne. A Proposed New Biomechanical Head Injury Assessment Function - The Maximum Power Index. 44th Stapp Car Crash Conference . 2000. Atlanta, Georgia, SAE.
- [25] J. Newman, C. Barr, M. Beusenbergh, E. Fournier, N. Shewchenko, E. Welbourne and C. Withnall. A New Biomechanical Assessment of Mild Traumatic Brain Injury - Part 1 - Methodology. Proceedings of IRCOBI Conference . 1999. Barcelona, Spain.
- [26] T.Gennarelli, F.Pintar and N.Yoganandan. Biomechanical tolerances for diffuse brain injury and a hypothesis for genotypic variability in response to trauma. 2003. Annual proceeding AAAM.
- [27] F. Feist, S. Faßbender, R. Puppini, E. Mayrhofer, T. Smith and J. Gugler. Impact situations and pedestrian/cyclist kinematics based on real world accident scenarios. Deliverable report for APROSYS WP2.1 AP-SP21-0069 D211B, 1-135. 18-4-2006. European Commission.
- [28] Emma Carter, Steve Ebdon and Clive Neal-Sturgess. Optimization of Passenger Car Design for the Mitigation of Pedestrian Head Injury Using a Genetic Algorithm. 2005. Genetic And Evolutionary Computation Conference, Association for Computing Machinery.
- [29] Madymo Theory Manual - Release 6.4.1, pp. 1-400, 2007.
- [30] Koji Mizuno and Janusz Kajzer. Head Injury in Vehicle-Pedestrian Impact. SAE Paper 2000-01-0157 . 2000. SAE 2000 World Congress.
- [31] Lex van Rooij, Kavi Bhalla, Mark U.Meissner, Johann Ivarsson, Jeff Crandall, Douglas Longhitano, Yukou Takahashi, Yasuhiro Dokko and Yuji Kikuchi. Pedestrian Crash Reconstruction using Multi-Body Modeling with Geometrically detailed, validated Vehicle Models and Advanced Pedestrian Injury Criteria. Proceedings of the 18th International Technical Conference on the Enhanced Safety of Vehicles (ESV) , 1-19. 2003.
- [32] S. Faßbender, M. Hamacher, R. Puppini, F. Feist and J. Gugler. AP-SP21-0077 D2.1.3 Demonstrator Module for New Design Concepts. 2007. Aachen, Deutschland, Institut für Kraftfahrzeugwesen (IKA), RWTH Aachen.
- [33] APROSYS WP 2.1. Hemisphere testing of MAN L-2000 cabin. Feist, F., Kassegger, H., and Mayrhofer, E. AP SP21 0056, 1-76. 15-4-2005. Graz, Austria, Vehicle Safety Institute, TU Graz.
- [34] T. Ziegenhain. Rechnergestützte Untersuchung mittels Mehrkörpermodell in PC-Crash 8.1 zum Zusammenhang zwischen Aufwurf- und Wurfweite eines Fußgängers. 1-119. 28-5-2008. Vehicle Safety Institute, Graz University of Technology.
- [35] Denis Wood and Ciaran Simms. Coefficient of Friction in Pedestrian throw. 12-14. 2000. Impact - Journal of ITAI, vol. 9 no 1.
- [36] C. K. Simms and D. P. Wood. The Effect of Pedestrian Motion on Head Contact Forces with Vehicle and Ground. Proceedings of IRCOBI Conference . 2005. Prague, Czech Republic.
- [37] S. Yoshida. Computer Simulation System for Car-Pedestrian Accident. Proceedings of the 16th International Technical Conference on the Enhanced Safety of Vehicles . 1998. Windsor, Canada.
- [38] Y.Mizuno. Summary of IHRA Pedestrian safety WG activities - Proposed test methods to evaluate pedestrian protection afforded by passenger cars. 2003. Japan Automobile Standards Internationalization Center.
- [39] Costin D.Untaroiu, Mark U.Meissner, J.Crandall, Yukou Takahashi, Masayoshi Okamoto and Osamu Ito. Crash reconstruction of pedestrian accidents using optimization techniques. 2008. International Journal of Impact Engineering.
- [40] T. J. Stevenson. Simulation of Vehicle-Pedestrian Interaction. 1-342. 2006. Canterbury, United Kingdom, University of Canterbury.
- [41] B. Chadbourn, D. Newcomb and D. Timm. Measured and Theoretical Comparisons of Traffic Loads and Pavement Response Distributions. Proceedings, 8th International Conference on Asphalt Pavements , 229-238. 1997. Seattle, Washington, USA.

- [42] P. Davich, J. Labuz, B. Guzina and A. Drescher. Small Strain and resilient modulus testing of granular soils. 2004-39, 1-117. 2004. Minneapolis, Minnesota, USA, University of Minnesota, Department of Civil engineering.
- [43] H. Salem and F. Bayomy. Predictopm of Seasonal Variation of the Asphalt Concrete Modulus using LTPP Data. 1-33. 2005. Moscow, Idaho, USA, University of Idaho.
- [44] K. Nesnas and B. Ferne. A theoretical evaluation of the use of the Falling Weight Deflectometer to predict stiffness. UPR/IE/212/06, 1-52. 2006. Crowthorne, UK, TRL Limited.
- [45] W. C. Young and R. G. Budynas, Roark's Formulas for Stress and Strain, pp. 1-854, McGraw-Hill, 2002.
- [46] D. P. Wood and C. K. Simms. Coefficient of friction in pedestrian throw. *Impact* 9 (1), 12-15. 2000.
- [47] A. Sacher. Slip Resistance and the James Machine 0.5 Static Coefficient of Friction-Sine Qua Non. *ASTM Standardization News* , 52-59. 1993.
- [48] R.W.G.Anderson, A.D.Long, T.Serre and C.Masson. Determination of boundary conditions for pedestrian collision reconstructions. *Proceedings of the ICrash Conference 2008* . 2008. Kyoto.
- [49] J. R. Wassermann and R. A. Koenigsberg. Diffuse Axonal Injury. *eMedicine - Medscape's Continually Updated Clinical Reference* . 26-7-2007.
- [50] F. Dimasi, R. Eppinger and F. Bandak. Computational analysis of head impact response under car crash loadings. *Proceedings 39th Stapp Car Crash Conference* , 425-438. 1995. SAE.
- [51] E. Takhounts and R. Eppinger. On the development of the SIMon finite element head model. *Proceedings 47th Stapp Car Crash Conference* , 107-133. 2003. SAE.
- [52] F. Bandak, A. X. Zhang, R. E. Tannous, F. Dimasi, P. Masielle and R. Eppinger. Simon: a simulated injury monitro; application to head injury assessment. *Proceedings of the 17th International Technical Conference on the Enhanced Safety of Vehicles (ESV)* . 2001. Washington, D.C., National Highway Traffic Safety Administraion.
- [53] S. Kleiven and W. Hardy. Correlation of an FE model of the human head with loacl brain motion - Consequence for injury prediction. *Proceedings 46th Stapp Car Crash Conference* , 123-144. 2002. SAE.
- [54] M. Gilchrist and T. J. Horgan. Influence of FE model variability in predicting brain motion and intercranial pressure changes in head impact simulations. *International Journal of Crashworthiness* 9, 401-418. 2004.
- [55] H. S. Kang, R. Willinger, B. Diaw and B. Chinn. Validation of a 3D anatomic huamn head model and replication of head impact in motorcycle accident by finiet element modelling. *Proceedings 41th Stapp Car Crash Conference* , 329-338. 1997. SAE.
- [56] R. Willinger and D. Baumgartner. Human head tolerance limits to specific injury mechanisms. *International Journal of Crashworthiness* 8, 605-617. 2003.
- [57] C. Deck, S. Nicolle and R. Willinger. Human head FE modelling: improvement of skull geometry and brain constitutive laws. *Proceedings of IRCOBI Conference (International Conference on the Biomechanics of Impact)* , 79-92. 2004. Graz, Austria.
- [58] R. Willinger, H. S. Kang and B. Diaw. 3D human head finite element model validation against two experimental impacts. *Annals of Biomed.Eng.* 27(3), 403-410. 1999.
- [59] T. Dziejowski, S. Bidal, P. J. Arnoux, C. Deck, R. Willinger, I. Ciglaric, F. Feist, M. Beaugonin and R. Meijer. Usage of human model in virtual testing of pedestrian impact - A virtual testing demonstrator and discussion. AP-SP53-0026, D5324, 1-68. 18-2-2008. European Commission. Aprosys Deliverable Reports.
- [60] P. Martin and R. Eppinger. Incidence of Head Injuries Attributable to rotation. *Proceedings of the 31st International Workshop on Injury Biomechanics* . 2002.
- [61] P. Prasad and H. J. Mertz. The position of the United States Delegation to the ISO Working Group 6 on the use of HIC in the automotive environment. *SAE Transactions*, Vol.94 . 1984. SAE International, Warrendale, Pennsylvania, USA.
- [62] World Health Organisation and German Insitute of Medical Documentation. *International Statistical Classification of Diseases and Related Health Problems, 10th Revision, Version for 2007*. <http://www.who.int/classifications/apps/icd/icd10online/> . 2007. 13-3-2009.
- [63] V. Barell and E. MacKenzie. The Barell Injury Diagnosis Matrix - Classification by Body Region and Nature of the Injury. http://www.cdc.gov/nchs/data/ice/final_matrix_post_ice.pdf . 1-11-2005. 1-3-2009.
- [64] J. Yang, *Review of injury biomechanics in car-pedestrian collisions*. *Int J Vehicle Safety I, Nos.1/2/3*, 100-117 (2005).
- [65] C.Arregui. Rotational acceleration as a traumatic brain injury mechanism in pedestrian-vehicle collisions. Doctoral dissertation . 2005. Polytechnic University of Cataluna.
- [66] A. Ommaya, *Biomechanics of head injury*. In *Biomechanics of Trauma*. (Ed. A. M. Nahum and J. W. Melvin) Appleton-Century-Crofts, Norwalk 1984.
- [67] J. Yang, J. Yao and D. Otte. Correlation of Different Impact Conditions to the Injury Severity of Pedestrians in Real World Accidents. *Proceedings of the 19th International Technical Conference on the Enhanced Safety of Vehicles (ESV)* . 6-6-2005. Washington DC, USA.
- [68] D. Otte and T. Pohlemann. Analysis and Load Assessment of Secondary Impact to Adult Pedestrians After Car Collisions on Roads. *Proceedings of IRCOBI Conference (International Conference on the Biomechanics of Impact)* . 2001. Isle of Man, UK.
- [69] K. Tanno, M. Kohno, N. Ohashi, K. Ono, K. Aita, H. Oikawa, M. T. Oo, K. Honda and S. Misawa. Patterns and Mechanisms of Pedestrian Injuries Induced by Vehicles with Flat-Front Shape. *Legal Medicine* 2(2), 68-74. 2000.
- [70] J. W. Garrett. An analysis of fatal pedestrian accidents. *SAE International Congress and Exposition* . 23-2-1981. Detroit, Michigan, USA, SAE International, Warrendale, Pennsylvania, USA.